Acetylcholinesterase Clustering at the Neuromuscular Junction Involves Perlecan and Dystroglycan

H. Benjamin Peng,*‡ Hongbo Xie,* Susanna G. Rossi,*§ and Richard L. Rotundo*§

*Department of Cell Biology and Anatomy and ‡Curriculum in Neurobiology, University of North Carolina, Chapel Hill, North Carolina 27599-7090; and §University of Miami School of Medicine, Miami, Florida 33136

Abstract. Formation of the synaptic basal lamina at vertebrate neuromuscular junction involves the accumulation of numerous specialized extracellular matrix molecules including a specific form of acetylcholinesterase (AChE), the collagenic-tailed form. The mechanisms responsible for its localization at sites of nerve–muscle contact are not well understood. To understand synaptic AChE localization, we synthesized a fluorescent conjugate of fasciculin 2, a snake α-neurotoxin that tightly binds to the catalytic subunit. Prelabeling AChE on the surface of *Xenopus* muscle cells revealed that preexisting AChE molecules could be recruited to form clusters that colocalize with acetylcholine receptors at sites of nerve–muscle contact. Likewise, purified avian AChE with collagen-like tail, when transplanted to *Xenopus* muscle cells before the addition of nerves, also accumulated at sites of nerve–muscle contact. Using exogenous avian AChE as a marker, we show that the collagenic-tailed form of the enzyme binds to the heparan-sulfate proteoglycan perlecan, which in turn binds to the dystroglycan complex through α-dystroglycan. Therefore, the dystroglycan–perlecan complex serves as a cell surface acceptor for AChE, enabling it to be clustered at the synapse by lateral migration within the plane of the membrane. A similar mechanism may underlie the initial formation of all specialized basal lamina interposed between other cell types.

Key words: acetylcholinesterase (AChE) • neuromuscular junction • perlecan • heparan-sulfate proteoglycan • dystroglycan • basal lamina

ACETYLCHOLINESTERASE (AChE)[1] is concentrated at the vertebrate neuromuscular junction (NMJ), tightly associated with the synaptic basal lamina, where it is responsible for terminating neurotransmission (43). This highly localized accumulation of AChE is a conspicuous marker for the specialization of the junctional extracellular matrix (ECM) that accompanies acetylcholine receptor (AChR) accumulation and synapse formation (44). Despite considerable progress in understanding the process of AChR clustering at this synapse, little is known about the mechanism(s) responsible for the accumulation of AChE and other components of the synaptic basal lamina. As an integral membrane protein, the AChR undergoes lateral movement within the plane of the cell membrane to become clustered at sites of nerve–muscle contact as a result of its association with the postsynaptic cytoskeleton (35). The synaptic AChE, on the other hand, is an ECM-bound protein thus can not on its own associate with the postsynaptic cytoskeleton for clustering. Except for the observations that several specific components of the synaptic basal lamina cocluster with AChR (reviewed in 25), little is known about how these molecules interact with each other as well as how they become associated with the neuromuscular synapse.

The predominant form of AChE at the NMJ is the asymmetric, or A12, form consisting of three tetramers of catalytic subunits covalently-linked to a collagen-like tail (43). This form is tightly attached to the synaptic basal lamina via its collagen-like tail and cannot be removed using chaotropic agents such as 8 M urea or 4 M guanidine HCl (52). Only proteolysis can effectively remove the AChE from the synaptic basal lamina (7, 24). The collagen-like tail can bind to heparin and this property appears to be essential for the localization of this enzyme on the muscle cell surface and its concentration at the NMJ (30, 53, 56). Bacause heparan sulfate proteoglycan (HSPG)

Address correspondence to Dr. H. Benjamin Peng, Department of Cell Biology and Anatomy, University of North Carolina, CB#7090, Chapel Hill, NC 27599. Tel.: (919) 966-1338. Fax: (919) 966-1856. E-mail: unchbp@med.unc.edu

1. *Abbreviations used in this paper:* AChE, acetylcholinesterase; AChR, acetylcholine receptor; BTX, α-bungarotoxin; DG, dystroglycan; ECM, extracellular matrix; HB-GAM, heparin-binding growth-associated molecule; HSPG, heparan-sulfate proteoglycan; MTJ, myotendinous junction; NMJ, neuromuscular junction; OG-BTX, Oregon green-conjugated α-bungarotoxin; R-fasciculin 2, tetramethylrhodamine-conjugated fasciculin 2; RU, resonance units.

is concentrated at the NMJ (3, 6, 57), it has been suggested that this property of A12 AChE may underlie its synaptic clustering (53).

By labeling cultured muscle cells with rhodamine-conjugated fasciculin 2 (R-fasciculin 2), a new fluorescent probe for AChE, before the addition of synaptogenic stimuli such as spinal cord neurons or growth factor-coated beads, we have found that preexisting cell surface AChE molecules become clustered at the site of postsynaptic development. To identify molecules responsible for synaptic AChE localization, we transplanted quail AChE to cultured *Xenopus* muscle cells and visualized it using a species-specific monoclonal antibody. The asymmetric form of AChE (A12), but not the globular forms (G2/G4), bind to and colocalizes precisely with perlecan, a major modular HSPG in skeletal muscle (32, 50). Perlecan itself binds to dystroglycan (DG), a transmembrane protein complex that interacts with molecules in the extracellular matrix such as laminin and agrin as well as with the cytoskeleton (28, 50). Both perlecan and DG become clustered at the postsynaptic membrane during NMJ formation (50). These data are consistent with our in vivo observations that endogenous AChE, detected with R-fasciculin 2, colocalizes precisely with perlecan and DG and suggest that AChE, via a transmembrane protein complex consisting of HSPG and DG, can be clustered by lateral migration, followed by anchorage to the postsynaptic cytoskeletal scaffold.

Materials and Methods

Materials

Fasciculin 2 was obtained from Sigma Chemical Co. and α-bungarotoxin (BTX) was purchased from Biotoxins, Inc. Tetramethylrhodamine-conjugated fasciculin 2 and Oregon green 488-conjugated BTX were prepared using the corresponding FluorReporter Protein Labeling Kit (Molecular Probes) following the manufacturer's recommended procedures and the unreacted dyes removed using BioGel P-2 spin columns (Bio Rad Laboratories). Heparin (cat. no. H-2149) was obtained from Sigma Chemical Co.

Isolation and Purification of Quail AChE Forms

The globular and collagenic-tailed AChE forms were isolated from tissue-cultured quail myotubes by detergent/high salt extraction followed by preparative sucrose gradient sedimentation as previously described (55). The pooled fractions from several gradients containing the G4 tetramers and the G2 dimers (globular forms) or A12 collagenic-tailed AChE forms were purified on an immunoaffinity column containing mAb 1A2 anti-avian AChE antibody (54) covalently attached to Sepharose CL-4B at a concentration of 1 mg/ml. The bound AChE was eluted with 0.1 M triethylamine, pH 11, in 1 M NaCl and 0.5% Triton X-100, and neutralized with Tris-HCl to pH 7. The AChE concentration was estimated using radiometric assay (33).

Cell Culture and Labeling

The myotomal region of *Xenopus laevis* embryos was excised and dissociated to make muscle cultures according to a previously published method (47). To induce the formation of clusters of AChR or AChE, muscle cells were cocultured with spinal cord neurons to establish the NMJ, or treated with 10-μm polystyrene latex beads coated with recombinant heparin-binding growth-associated molecule (HB-GAM) which also induces the formation of postsynaptic specializations (49). To visualize endogenous AChE, muscle cultures were labeled with R-fasciculin 2 at a concentration of 150 nM for 0.5–1 h and then examined by fluorescence microscopy either in the living state or after fixation with 95% ethanol at −20°C. For most experiments, the cultures were double-labeled with OG-BTX (at 150 nM) to visualize AChRs. To study the binding of exogenous AChE to the surface of *Xenopus* muscle cells, cultures were incubated with either purified quail A12 collagenic-tailed AChE (at 0.1–0.2 ng/ml) or G2/G4 globular forms of AChE (at 0.5 ng/ml) for 1 h. The transplanted quail AChE was then examined by labeling *Xenopus* cultures with mAb 1A2 followed by fluorescently conjugated secondary antibody. HSPG at the cell surface was detected with mAb HepSS-1, an anti-heparan sulfate monoclonal antibody (Seikagaku Corp.). A polyclonal anti-perlecan antibody (27), a generous gift of Dr. J. Hassell (Shriners Hospitals for Children, Tampa, FL), was used to label this HSPG in *Xenopus* cells. The localization of DG was studied with a monoclonal anti–β-DG antibody (Novacastra Laboratories). The HSPG and perlecan labeling was done on live cultures, but the DG labeling was carried out after cell fixation and permeabilization since the antibody recognizes an intracellular epitope of the transmembrane protein. To label *Xenopus* myotomal muscle fibers in vivo, the tail of the larva was skinned, fixed, and incubated with the antibody. Alternatively, the fibers within the tail musculature were first dissociated with collagenase and then immunolabeled.

Binding of AChE Forms to Perlecan: Sepharose Bead Assay

Purified anti-avian perlecan antibody mAb 33 (6) was prepared from ascites fluid obtained by using the original hybridoma cell line (a generous gift from Dr. Douglas M. Fambrough, Johns Hopkins University, Baltimore, MD). The purified antibody was absorbed onto protein A–Sepharose CL-4B beads (Sigma Chemical Co.) to saturation, and the beads washed extensively to remove unbound antibody. The beads were then used to capture perlecan secreted by quail myotube cultures. Myotube-conditioned medium from 5-d-old cultures was centrifuged 30 min at 12,000 *g* and 500-μl aliquots of supernatant were incubated with 10 μl of the mAb 33 beads overnight. After extensive washing with PBS containing 5 mM EDTA and 0.5% BSA, the beads were treated with 1 μM diisopropylfluorophosphate to irreversibly inhibit any trace amounts of endogenous AChE already bound to perlecan. After washing with PBS, EDTA, and BSA, aliquots of immobilized perlecan beads were diluted in microfuge tubes with 500 μl PBS, 0.5 M NaCl, 1 mM EDTA, 0.5% BSA, and 0.5% Triton X-100 containing either 0.1–0.2 ng purified A12- or G4/G2-AChE or buffer alone. After 1-h incubation at 5°C, the salt concentration was decreased to 0.3 M NaCl and incubation continued overnight. The next day the beads were washed three times with PBS, 5 mM EDTA, and 0.5% BSA and assayed for AChE activity using a radiometric assay as previously described (54).

Binding of AChE Forms to Perlecan: BIAcore assay

AChE-perlecan binding was also assayed by the surface plasmon resonance biosensor technology (42). A BIAcore X instrument (BIAcore. Inc.) was used in this study. Perlecan purified from Englebreth-Holm-Swarm tumor (37), kindly provided by Dr. J. Hassell (Shriners Hospitals for Children, Tampa, FL), was conjugated to BIAcore sensor chip CM5 with carboxylated dextran surface. The chip surface was first treated with a mixture of *N*-hydroxysuccinimide (NHS, 50 mM) and 1-ethyl-3-(3-dimethylaminopropyl) carbodiimide (EDC, 200 mM) in Hepes-buffered saline (HBS, 10 mM Hepes, 150 mM NaCl, 3 mM EDTA, and 0.005% surfactant P20, pH 7.4). After washing with HBS, the perlecan sample, diluted to a concentration of 30 ng/ml with 100 mM Na-acetate buffer at pH 5, was injected into the flow cell to effect coupling and this process was terminated with 1 M ethanolamine (pH 8.5). Samples were then injected into the flow cell to study their binding to perlecan. Globular G2/G4 AChE was diluted to a concentration of 10 ng/ml and asymmetric A12 AChE was diluted to 2.3 ng/ml with HBS immediately before injection and 20 μl of each sample was injected into the flow cell. The change in resonance units (RU), indicative of the binding and dissociation, was continuously recorded with a computer. The data were analyzed with BIAevaluation software supplied by the manufacturer and plotted with SigmaPlot software (SPSS, Inc.).

Results

Distribution of AChE on Xenopus Muscle Visualized with Fluorescent Fasciculin 2

Fasciculin 2, a 61–amino acid snake α-neurotoxin isolated from the venom of African mambas, binds specifically and

tightly to the catalytic subunit of AChE (9, 34). The crystal structure of the AChE-fasciculin 2 complex has been determined and the molecular interactions between the toxin and the enzyme are well characterized (9, 19, 26). To study the distribution and fate of AChE, we synthesized a tetramethylrhodamine conjugate of fasciculin 2 to label the enzyme on muscle cells. When the cutaneous pectoris muscle of the frog (*Rana pipiens*) was double-labeled with R-fasciculin 2 and OG-BTX, a precise colocalization pattern of AChE and AChR was observed. Fig. 1, A and B show a single muscle fiber imaged in whole mount. Like AChRs, AChE labeling also exhibits a banding pattern typical of the frog NMJ. Detailed analyses of the R-fasciculin 2 labeling pattern by conventional and confocal microscopy have shown a more precise registration of AChE and AChR at the NMJ than the pattern hitherto observed with histochemical or immunocytochemical methods (Rotundo, R.L., and H.B. Peng, manuscript in preparation).

Since *Xenopus* myotomal muscle cells were used to study AChE clustering in this study, we also examined AChE distribution in the tail musculature of the larva with R-fasciculin 2. As shown in Fig. 1 (C and D), R-fasciculin 2 labeling was colocalized with sites of AChR clustering at NMJs revealed by OG-BTX labeling. In addition to the NMJ, R-fasciculin 2 also labeled myotendinous junctions (MTJs) which are located adjacent to the NMJs at the intersomitic area (Fig. 1, E and F). The MTJ labeling showed up as a series of streaks oriented longitudinally at the ends of the myotome. These streaky structures correspond to membrane invaginations where myofibrils insert into the sarcolemma (13, 46). This MTJ localization of AChE revealed by R-fasciculin 2 is consistent with previous histochemical results (16, 41).

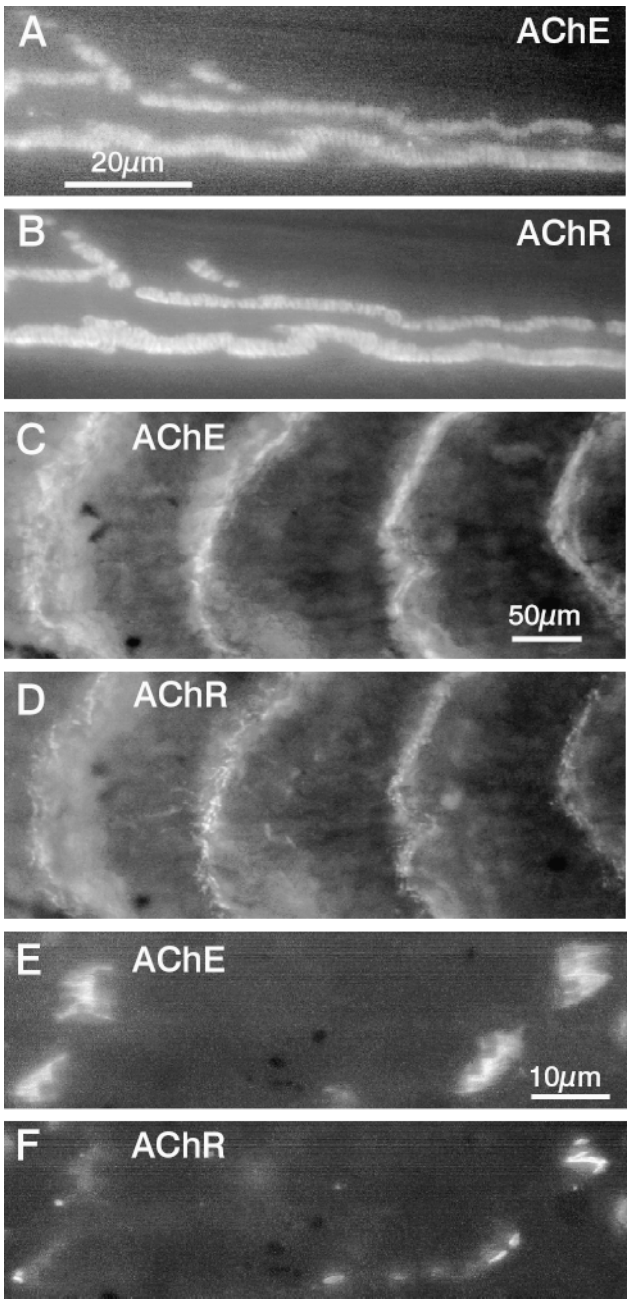

Figure 1. Distribution of AChE in skeletal muscle revealed by fluorescent fasciculin 2 labeling. The cutaneus pectoris muscle of *Rana pipiens* was double-labeled with R-fasciculin 2 (A) and OG-BTX (B) in whole mount and single fibers were isolated for observation. Colocalization of AChE and AChR is observed. Like AChRs, the distribution of AChE molecules exhibits the characteristic banding pattern associated with the junctional folds. (C–F) R-fasciculin 2 and OG-BTX labeling of *Xenopus* larval myotomal muscle. AChE is concentrated at both ends of the myotomal muscle fibers (C) where AChRs are also clustered as shown by OG-BTX labeling (D). (E) At higher magnification, the details of AChE localization are resolved. The enzyme is present both at the NMJ, marked by AChR labeling (F), and at the MTJ as shown by the streaky R-fasciculin 2 labeling pattern (E) which corresponds to deep membrane invaginations at this sarcolemmal specialization.

Clustering of Endogenous AChE Studied with R-Fasciculin 2

To study the clustering of AChE, cultured *Xenopus* myotomal muscle cells were labeled with R-fasciculin 2. As shown in Fig. 2 (A and B), R-fasciculin 2 labeling was observed at spontaneously formed AChR clusters on these muscle cells, and the pattern of AChE labeling closely resembled that of the AChR. Virtually all AChR hot spots observed were associated with AChE. Previous studies have shown that AChR clusters at the NMJ are derived, at least in part, from the preexisting pool of cell surface receptors by lateral migration (2). To determine whether preexisting AChE molecules could also contribute to synaptic clusters, muscle cells were prelabeled with R-fasciculin 2 and then cocultured with spinal cord neurons or treated with beads coated with HB-GAM, which mimic the nerve in inducing postsynaptic specializations (49). As shown in Fig. 2, preexisting AChE labeled with R-fasciculin 2 became concentrated at bead-induced AChR clusters (C and D) and at the developing NMJ (F–H) marked by OG-BTX. These results were based on observations made on a total of six separate nerve–muscle and bead–muscle cocultures encompassing >100 cell pairs each. Consistently, AChE clustering as evidenced by R-fasciculin 2 labeling was detected at a much smaller percentage of nerve- or bead-induced AChR clusters in 1-d cocultures

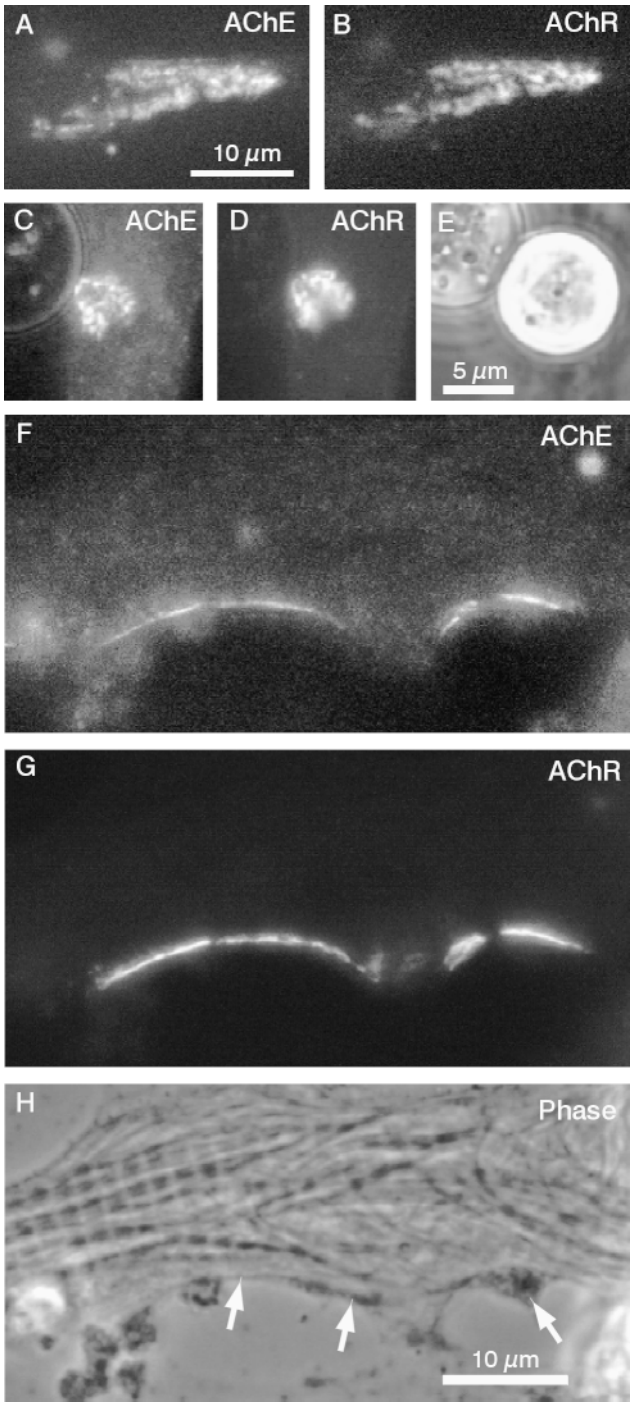

Figure 2. AChE clustering in cultured *Xenopus* muscle cells. (A and B) A spontaneously formed hot spot of AChE and AChR visualized by R-fasciculin 2 and OG-BTX labeling. (C–E) An AChE cluster induced by a HB-GAM–coated bead. The culture was prelabeled with R-fasciculin 2 and OG-BTX before bead application. Thus, this cluster was formed from preexistent AChE and AChR. (F–H) Clustering of preexistent AChE at the NMJ. The muscle culture was innervated with spinal cord neurons after prelabeling with fluorescent toxins. Both AChE and AChR become clustered at sites of nerve–muscle contact (indicated by arrows in H) formed along the length of this neurite.

(~20%) than in 2-d cocultures (>70%). This suggests that AChE clustering lags behind AChR clustering by ~1 d.

The fluorescence intensity of R-fasciculin 2 labeling at the cluster was generally several-fold less than that of the corresponding OG-BTX labeling when each was normalized with respect to the background. This suggests that the site density of AChE at the cluster is significantly less than that of the receptor. Since AChE is a secreted molecule, it is possible that most of the molecules are secreted into the medium and not captured by the cell surface acceptors (to be described below) in tissue culture. Alternatively, it is possible that not all AChE molecules are available for fasciculin 2 labeling, and that the toxin's affinity for AChE decreases with time.

More importantly, however, these data show that, like AChRs, preexisting cell surface AChE molecules can be recruited to form clusters and suggest that they are capable of undergoing lateral migration at the cell surface to become aggregated at sites of synaptic stimulation.

Transplantation of Exogenous AChE onto Xenopus Muscle Cells: Colocalization with Perlecan

To identify the molecules on the cell surface that can serve as acceptors for AChE during the process of synaptic localization, we transplanted exogenous AChE to cultured *Xenopus* muscle cells by adapting a method previously used to study the localization of this enzyme at the NMJ in vivo (56). The collagenic-tailed A12 AChE form or the globular AChE forms consisting of dimers (G2) and tetramers (G4) of catalytic subunits were purified from cultured quail myotubes and applied to cultured *Xenopus* muscle cells at a concentration of 0.1–0.4 ng/ml. Their binding to the cell surface was then detected with mAb 1A2 which specifically labels the catalytic subunit of quail AChE but not the *Xenopus* enzyme (54, 56).

The transplanted collagenic-tailed A12 form of AChE bound to the surface of *Xenopus* muscle cells in a clustered manner (Figs. 3 A and 4 A), where they often colocalized with AChR hot spots (Fig. 4, A and B), or sometimes more diffusely (Figs. 3 C). Although the pattern of the AChE clusters bore similarity to that of AChRs, they were not congruent with each other. The AChE cluster generally occupied a larger area than the AChR cluster. As it is known that the A12 AChE binds to heparin via its collagen-like tail to be sequestered on the muscle cell surface and at the NMJ (30, 53, 56), we examined whether transplanted A12 AChE was associated with HSPG on the cell surface. Pretreatment of muscle cells with heparin at a concentration of 20 μg/ml abolished the binding of A12 AChE to the cell surface (data not shown). Perlecan is an abundant HSPG on the surface of skeletal muscle and appears to play an important role in muscle differentiation (31, 45, 50, 51). We thus examined its relationship to AChE. Although this molecule is generally considered as an ECM-bound HSPG, our recent study has shown that a pool of perlecan is actually associated with the cell membrane by interacting with α-DG in skeletal muscle cells (50). In fact, the bulk of perlecan on cultured *Xenopus* muscle cells is cell membrane-associated since these cells secret relatively small amount of matrix molecules and do not form organized basal lamina under culture conditions

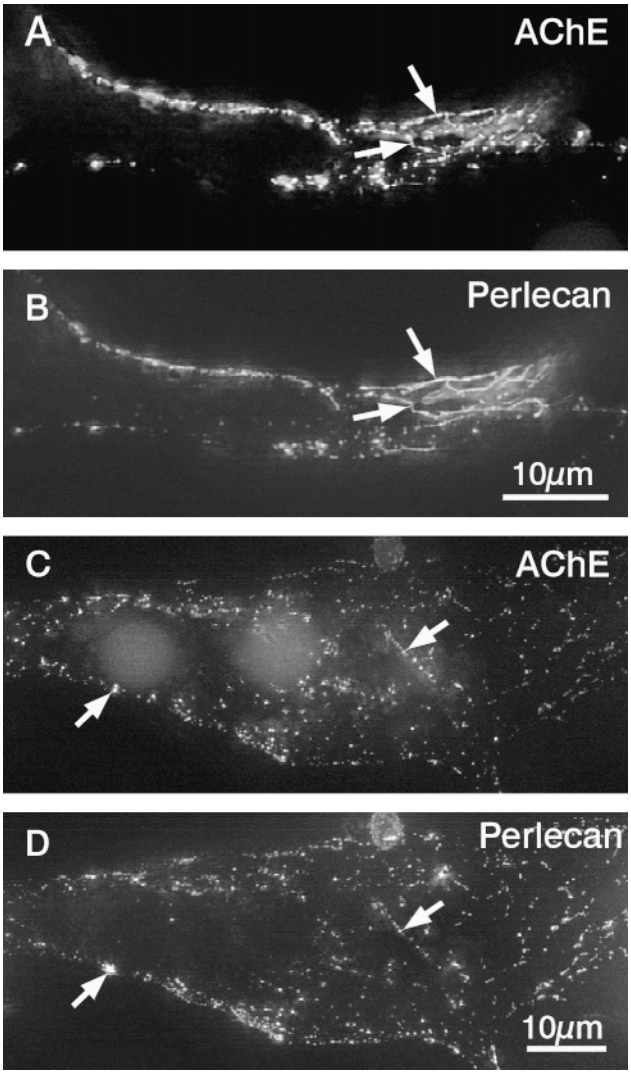

Figure 3. Transplantation of quail AChE onto *Xenopus* muscle cells. Cultured *Xenopus* muscle cells were incubated with collagenic-tailed quail A12 AChE and its binding to the cell surface detected with avian AChE-specific mAb 1A2. Transplanted AChE colocalized with perlecan on the cell surface in both the clustered (A and B) and diffuse states (C and D). Arrows point to the precise correspondence between the AChE and perlecan labeling.

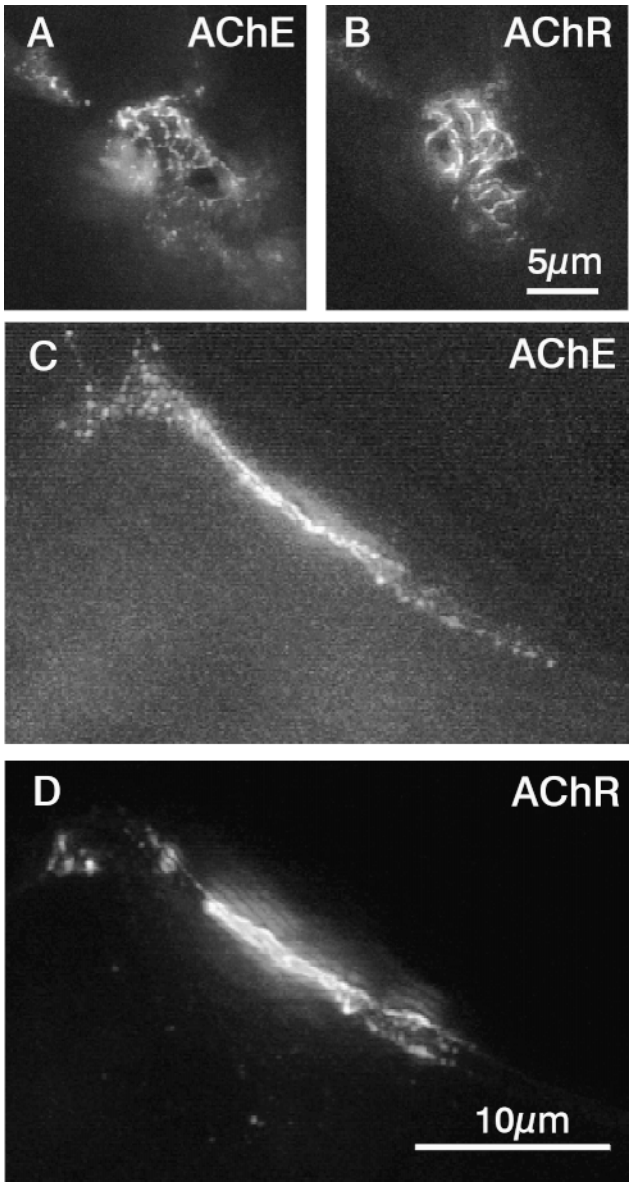

Figure 4. Transplanted collagenic-tailed AChE is enriched at AChR clusters. (A and B) Attachment of A12 AChE to sites of AChR accumulation on *Xenopus* muscle cells. (C and D) Clustering of transplanted A12 AChE at the NMJ. After the muscle culture was treated with exogenous AChE, it was innervated by spinal neurons to induce NMJ formation. This AChE, detected by mAb 1A2, becomes clustered at the developing NMJ.

of this study. To determine whether AChE codistributed with perlecan, anti-avian AChE mAb 1A2 and a polyclonal anti-perlecan antibody (27) were used to double-label A12 AChE-treated muscle cells (Fig. 3, A–D). Both clustered and diffusely distributed quail A12 AChE molecules were precisely colocalized with perlecan. In the clustered state (Fig. 3 A, B), the patterns of AChE and perlecan labeling coincided nearly perfectly while even in the diffuse state (Fig. 3, C and D), the puncta of labeling by these two antibodies also showed precise registration. These data, based on six transplantation experiments, thus strongly suggest that A12 AChE binds to perlecan.

In contrast to A12 AChE, globular G2/G4 AChE forms, which do not have the collagen-like tail and do not interact with HSPGs, showed little binding to the cell surface when applied at similar concentrations (Fig. 5). Moreover, the binding of these globular AChE forms bore no relationship to the pattern of perlecan labeling on the cell surface (Fig. 5, A and B).

Purified A12 AChE Binds to Perlecan via its Collagen-like Tail

To determine whether AChE could bind directly to perlecan, purified A12 or globular G2/G4 AChE forms were incubated with perlecan immobilized on mAb 33-conjugated

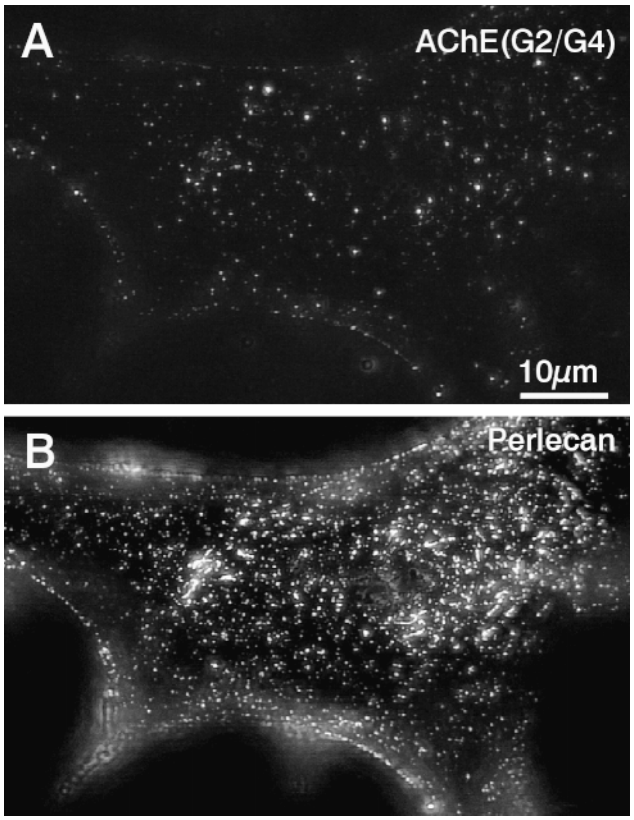

Figure 5. Nonspecific binding of globular G2/G4 forms of quail AChE to *Xenopus* muscle cells. The AChE was detected with mAb 1A2 (A) and the cell was double-labeled with anti-perlecan antibody (B). In comparison to A12 AChE, these forms showed only low level, non-specific binding to the cell surface without any correlation with the perlecan labeling.

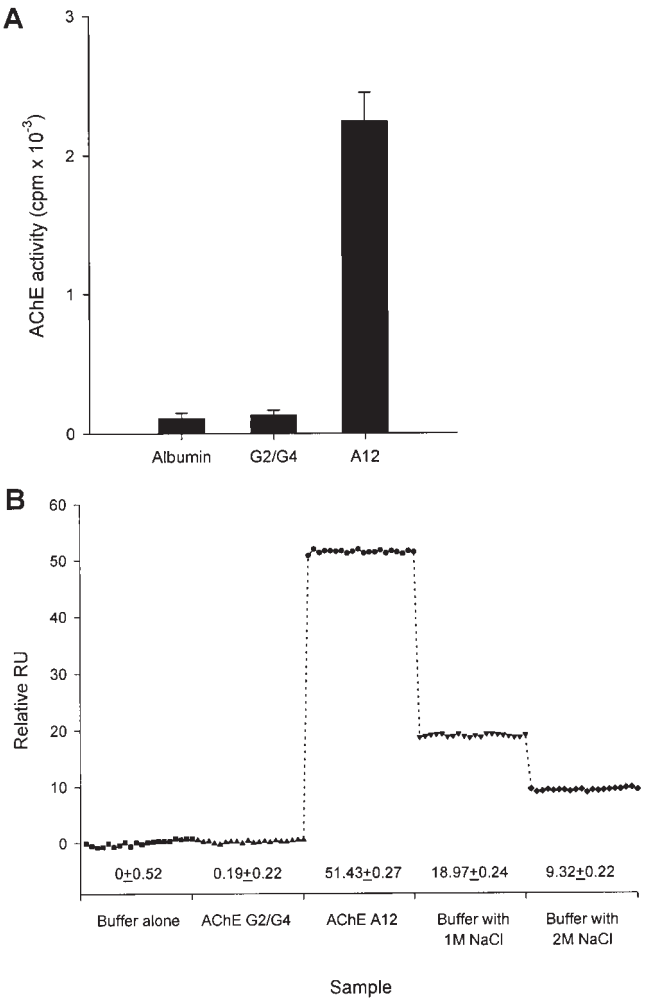

Figure 6. Binding of AChE to perlecan. (A) Binding of AChE to perlecan-conjugated Sepharose beads. Perlecan secreted by quail myotubes was captured on mAb #33-conjugated Sepharose beads which were then used to determine the binding of AChE to this HSPG. The AChE bound to the beads was quantified by radiometric assay. Only the collagenic-tailed A12 form of AChE exhibited strong binding to perlecan. The binding of the globular G2/G4 forms showed only background activity. (B) Binding assayed with BIAcore. Perlecan was covalently conjugated to a sensor chip and this surface was used to assess the binding of AChE. Samples were injected into the flow cell over the chip and the net change in RU at the termination of the sample injection and buffer wash was plotted. Using buffer injection as the baseline, G2/G4 AChE showed nearly no binding to perlecan. In contrast, A12 AChE showed strong binding, which was only reversed by high salt. The samples were injected sequentially as shown in the abscissa (from left to right). For each sample, the mean of 20 data points and the standard deviation are given at the bottom of the trace.

Sepharose beads. Beads incubated with bovine serum albumin, rather than perlecan-containing conditioned medium, were used as an additional control for nonspecific binding in these experiments. As shown in Fig. 6 A, the purified A12 AChE was bound to isolated perlecan. That the binding occurred in 0.3 M NaCl, which was necessary to prevent aggregation of the A12 AChE, suggests that it is with high affinity. In contrast, the globular G2/G4 oligomeric forms showed binding levels similar to the albumin control.

It could be argued that A12 AChE binds indirectly to the antibody-perlecan beads via other molecules in the conditioned medium. Thus, a second set of binding studies using surface-plasmon resonance (BIAcore) technology was conducted. In these experiments, purified perlecan was covalently linked to the sensor chip. Samples of G2/G4 and A12 AChE were then injected into the experimental chamber (flow cell) sequentially to study their interactions with the bound perlecan. In this assay, the binding is measured optically and expressed as the net increase in resonance units (RU) at the termination of sample injection. As shown in Fig. 6 B, buffer injection did not result in any increase in RU. Using this as a baseline, G2/G4 (at 0.2 ng in 20-μl sample volume) did not show any significant binding to perlecan. When A12 was injected (at 0.05 ng in 20-μl sample volume), a 270-fold change in RU over the G2/G4 value was seen, indicative of its binding to perlecan. This binding was not reversed by the running buffer that had 150 mM NaCl. Significant dissociation of A12 from the perlecan surface was only observed after a buffer with 1–2 M NaCl was injected into the flow cell as shown in Fig. 6 B.

These biochemical measurements thus show that A12 AChE binds directly to perlecan through its collagen-like tail and provide further support to our conclusion that cell surface perlecan serves as an acceptor for the synaptic A12 form of AChE. They are consistent with the cellular binding studies described above (Figs. 3 and 5). The fact that these two molecules are only dissociated under high salt condition is consistent with the notion that the binding is mediated by the heparan-sulfate glycosaminoglycan chains on perlecan.

Neurons Induce Clustering of Transplanted Avian AChE to Sites of Nerve–Muscle Contact

To determine whether the transplanted AChE can be recruited to form clusters at the NMJ, we innervated muscle cells pretreated with quail A12 AChE. As shown in Fig. 4 (C and D), this exogenous AChE was also clustered at developing NMJs revealed by R-BTX labeling. Again, the organization of the AChE cluster was not precisely aligned with that of the AChR clusters with the AChE cluster generally occupying a larger area than the AChR cluster. In contrast to the endogenous AChE, the NMJ localization of the transplanted AChE was clearly detectable in 1-d nerve–muscle cocultures (see Discussion). Thus, similar to endogenous AChE, the transplanted AChE can also be clustered by lateral migration at the cell surface.

The Role of Perlecan and Dystroglycan in AChE Clustering

Accompanying the clustering of AChE, HSPGs also became concentrated at the NMJ (3, 6, 50). To determine whether preexisting perlecan molecules can undergo lateral migration and become clustered, cultured muscle cells were labeled with anti-perlecan antibody and then treated with HB-GAM–coated beads followed by fluorescently conjugated secondary antibodies. As shown in Fig. 7 (A and B), preexistent perlecan was indeed clustered in response to the bead stimulation. Together with AChE binding to perlecan described above, these results suggest that the AChE-perlecan complex at the cell surface can be recruited to form synaptic clusters. As neither AChE nor perlecan is a transmembrane protein, an integral membrane linker for this complex would be necessary to effect its lateral migration at the cell surface.

The core protein of perlecan contains three globular domains at its COOH terminus that are also shared by laminin A-chain and agrin (32). Recently, we have shown that, like laminin and agrin, perlecan can bind directly to α-DG which is the extracellular component of the transmembrane DG glycoprotein complex and that these two proteins cocluster in response to synaptic stimuli such as spinal neurons and HB-GAM–coated beads (50). An example of this coclustering induced by beads is shown in Fig. 7 (C and D). Here both perlecan and DG become clustered at the bead–muscle contact and there is a high degree of registration between clusters of these two molecules. To determine whether AChE was also colocalized with DG, we double-labeled bead-treated muscle cells and nerve–muscle cocultures with R-fasciculin 2 and anti–β-DG antibody. As shown in Fig. 8, AChE and DG also appeared to be precisely coclustered at sites of nerve–muscle contacts (A and B) and at bead-induced clusters (C and D).

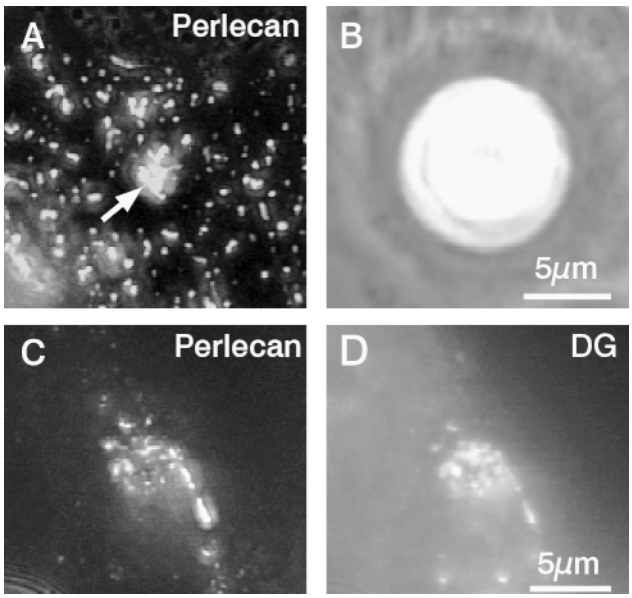

Figure 7. Clustering of preexistent perlecan induced by HB-GAM–coated beads. The muscle cell was prelabeled with anti-perlecan antibodies, treated with HB-GAM–coated beads, and then labeled with fluorescent secondary antibody 24 h later (A and B). (A) Distribution of perlecan at site of bead contact; (B) localization of HB-GAM–coated bead. All sites of perlecan accumulation at sites of bead contact (C) also showed accumulation of DG (D).

To correlate these data obtained from cultured muscle cells with AChE clustering in vivo, we examined the relationship between AChE, perlecan, and DG in whole mounts of myotomal muscle. As shown in Fig. 9 (A and B), AChE and perlecan are colocalized at both the NMJ and the MTJ. Double-labeling myotomal muscle with anti–β-DG antibody and fluorescent BTX revealed that DG is also clustered at the MTJ in addition to its being present at the postsynaptic membrane (Fig. 9, C and D). Finally, double-labeling myotomal muscle with β-DG antibody and R-fasciculin 2 showed colocalization of DG and AChE at intersomitic junctions (Fig. 9, E and F). At higher magnification, the colocalization of these two molecules at ends of the muscle fiber, where NMJs are located, and along MTJ invaginations became more evident (Fig. 9, G and H).

These data thus suggest that the perlecan-DG complex can serve as an acceptor for the collagenic-tailed form of AChE and allow it to assume an association with the muscle membrane. This membrane association may provide the structural basis for the observed clustering of preexistent membrane-bound AChE to the synaptic site.

Discussion

In this study, we used fluorescently conjugated fasciculin 2 to follow the clustering of AChE during NMJ formation. This probe has many of the same advantages as fluorescent α-bungarotoxin which has offered an extremely pow-

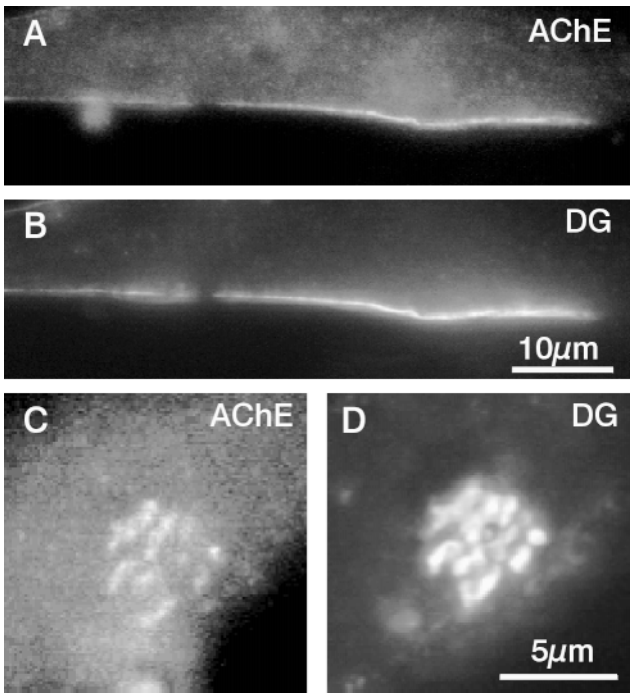

Figure 8. Colocalization of AChE and DG in culture. Endogenous AChE was labeled with R-Fasciculin 2 and DG was labeled with anti–β-DG antibody followed by FITC-conjugated second antibody. (A and B) Colocalization of AChE and DG at a NMJ. (C and D) Colocalization of AChE and DG at a bead–muscle contact.

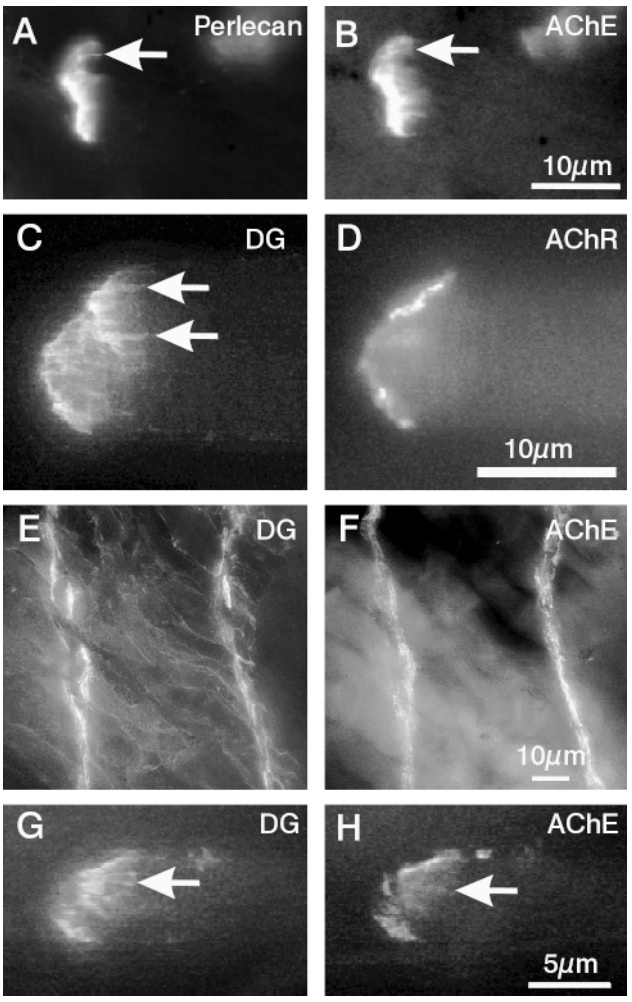

Figure 9. Colocalization of AChE, perlecan and DG on myotomal muscle fibers in vivo. (A and B) Perlecan and AChE colocalization at the ends of myotomal muscle fibers. Arrows point to the membrane invaginations of the myotendinous junction. (C and D) Clustering of DG at the NMJ, marked by AChR clusters (D) labeled with fluorescent α-bungarotoxin, and at the myotendinous junction (arrows). (E and F) Colocalization of DG and AChE at intersomitic junctions (low magnification). (G–H) Colocalization of DG and AChE at sarcolemma specializations shown at higher magnification. Arrows point to invaginations of the myotendinous junction.

erful tool for visualizing AChRs (1). Its compact size allows it to penetrate more deeply into tissues than antibody reagents. Its specificity and 1:1 stoichiometry in binding to the catalytic site of AChE (9) enables high-resolution imaging of AChE distribution on muscle cells. Iodinated fasciculin 2 has recently been used to quantify AChE site density in mammalian muscle by EM-autoradiography (4). To our knowledge, the current work is the first to utilize fluorescent fasciculin for optical imaging of AChE.

We have shown that a preexistent, membrane-bound collagenic-tailed form of AChE, either endogenously deposited or experimentally transplanted can be recruited to form clusters at the postsynaptic membrane. This suggests that AChE is capable of lateral migration on the cell surface and becomes immobilized at sites of synaptic differentiation. Thus, AChE clustering seems to bear similarity to the much studied AChR clustering process which can be explained by a diffusion-mediated trapping mechanism of AChRs preexistent on the cell surface (20, 35). Since AChE in muscle is not a membrane-bound protein, this necessitates one or more acceptor molecules to link it to the cell surface. The immunocytochemical colocalization and binding studies presented here show that perlecan is one such acceptor for A12 AChE. Perlecan is one of at least two modular HSPGs on the surface of skeletal muscle cells, the other being muscle agrin (32). Although the bulk of perlecan is associated with ECM, our recent studies have shown that a pool of this molecule is associated with the cell surface in association with α-DG (50). This work suggests that this cell surface pool is, at least in part, also involved in AChE anchorage. As AChE is secreted, this membrane-bound perlecan could readily capture and sequester it on the cell surface. This scheme is consistent with previous findings that the heparin-binding property of A12 AChE is essential for its localization on the cell surface (53). The heparin-binding motifs within the collagen-like tail of this AChE form have recently been elucidated (18, 36). The interaction between this motif and the heparan-sulfate side chain on the perlecan molecule seems to be the basis for the localization of this enzyme to the cell surface (53, 56). Despite our focus on perlecan, muscle agrin, which also becomes concentrated at sites of synaptic differentiation (38), may also be an acceptor for A12

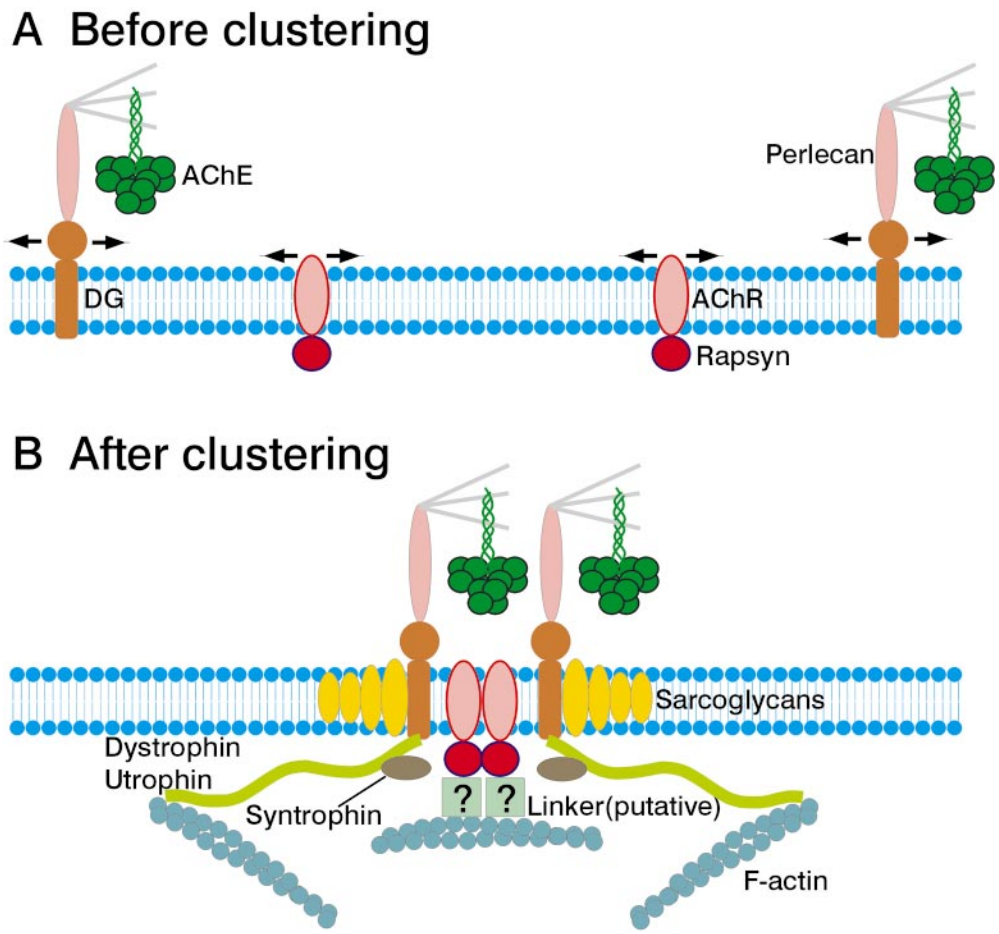

Figure 10. Model illustrating the involvement of the dystroglycan-perlecan complex in synaptic localization of the collagenic-tailed AChE form. (A) Before innervation, the COOH terminus of perlecan can interact with the transmembrane DG complex (50). The A12 collagenic-tailed AChE in turn binds to the heparan-sulfate chains of perlecan via its collagen-like tail. This association with a transmembrane protein complex enables the AChE to undergo lateral movement (arrows) on the cell surface in the similar manner as AChRs. (B) In response to innervation, the AChE-perlecan-DG complex is clustered by a mechanism similar to the lateral migration-mediated localization of AChRs. Other postsynaptic proteins, such as dystrophin, utrophin, syntrophin, and the sarcoglycan complex, as well as F-actin, may be involved in the formation and/or the stabilization of the cluster.

AChE. Our preliminary studies based on immunological labeling have shown that agrin can coexist with perlecan at the same loci on the cell membrane, albeit at a lower concentration.

Previous studies have shown that α-DG can interact with ECM-bound molecules that have G-domain motifs, such as laminin, agrin, and perlecan (10–12, 22, 28, 50, 58). On the other hand, β-DG, the transmembrane component of the DG complex, interacts with dystrophin or utrophin via its cytoplasmic tail (28). Thus, the DG complex is capable of mediating the transmembrane linkage between ECM and the cytoskeleton. This study suggests a new role for DG as a component of the machinery for cell surface sequestration and clustering of AChE and other ECM components in skeletal muscle during synaptogenesis as depicted in a model in Fig. 10. The transmembrane nature of the DG complex may allow it to undergo lateral movement within the plane of the membrane in the nonclustered state and thus to move its bound HSPG-AChE complex in a manner similar to the AChRs (Fig. 10 A). The lateral mobility of DG is also supported by the recent demonstration that exogenously applied laminin induces clustering of DG (15).

The mechanism for DG clustering at the synaptic site is unknown, although it may also be a cytoskeleton-mediated process as is the case of AChR clustering (8). For AChR clustering, there is compelling evidence to suggest that synaptogenic stimuli induce the formation of a postsynaptic cytoskeletal scaffold which serves to immobilize freely diffusing receptors. Lateral diffusion of AChRs, with a diffusion coefficient estimated to be on the order of 10^{-10}–10^{-9} cm^2/s, can account for the rate of AChR clustering induced by synaptogenic signal (35, 48). The cytoskeletal specialization underlying the postsynaptic membrane, including F-actin, utrophin/dystrophin, and the transmembrane sarcoglycan complex (25, 39) may be involved in the clustering and/or stabilization of the DG-HSPG-AChE complex (Fig. 10 B). The coclustering of AChE and AChR suggests that their clustering processes may share common determinants. Subtle differences, however, must also exist as shown by the lack of congruency between these two types of clusters with the AChE cluster being larger than the AChR cluster. In the same manner, it has been shown that clusters of dystroglycan and HB-GAM, which binds to HSPG, are also more extensive in area than AChR clusters despite their colocalization (14, 49).

Recent studies have shown that postsynaptic specializations, including both AChR and AChE clusters, still form in utrophin and dystrophin double-knockout mice despite their severe muscular dystrophy (17, 23). However, AChE appears to be "more scattered" according to one study (17). This could be due to two reasons. First, the postjunctional folds are greatly reduced in these animals. Because

synaptic AChE is associated with the basal lamina both on the top of and along the folds in normal muscle (44), their reduction should result in a significant deficit of AChE. Furthermore, the level of DG at the NMJ also seems to be reduced, although the exact level seems to vary between the two studies (17, 23). This could also reduce the total amount of AChE at the NMJ according our model. Nevertheless, the DG remaining at the NMJ may offer the structural basis of AChE localization even in these animals.

Our results have shown that the clustering of endogenous AChE lags behind that of AChRs by about a day in tissue culture. However, transplanted AChE becomes detectable at newly established NMJs on the same day as the AChRs. This suggests that the machinery for AChE clustering is activated at the time of synaptic stimulation, but other factors may limit the rate of AChE accumulation in cultured muscle cells. A previous study has shown that DG clustering is detectable on cultured *Xenopus* muscle cells within the first 1–2 h after nerve contact (14). Thus, the delay in AChE accumulation seems to be quantitative in nature due to the site density of this molecule on the muscle surface. As described above, the fluorescence intensity of R-fasciculin 2 labeling of AChE at clusters is generally much lower than that of AChR labeling. In fact, the site density of AChE at frog NMJ is estimated to be ~600 sites/μm^2 as compared with 10,000 sites/μm^2 for AChRs (5, 21). A factor that could limit the amount of membrane-bound AChE is the number of sites available for its binding on the heparan-sulfate chains of HSPGs. In addition to AChE, these chains also offer a substrate for other heparin-binding molecules such as several ECM components (59) and growth factors (49) for their localization at the cell surface. The low site density may thus account for the length of time necessary for its accumulation to detectable level at synaptic sites. Transplantation of exogenous AChE greatly increases its site density on the cell surface as shown by the visualization of diffusely distributed molecules (Fig. 3 C).

The clustering of AChE is an example of the specialization of synaptic basement membrane during NMJ formation. A recent study using DG-null embryoid bodies has shown that this protein plays a central role in the assembly of the basement membrane (29). In addition to AChE, the scheme presented in this work based on molecular interaction with HSPG-DG complex may also find application in the formation of other specializations involving heparin-binding synaptic molecules such as neuregulin and peptide growth factors (40, 49).

We thank Dr. Douglas Fambrough for the mAb 33 hybridoma, Dr. John R. Hassell for purified perlecan and its antibody, and Dr. Heikki Rauvala for recombinant HB-GAM.

This work was supported by National Institutes of Health grants NS-23583 (to H.B. Peng) and AG-05917 (to R.L. Rotundo) and by the Muscular Dystrophy Association (to H.B. Peng).

Received for publication 1 December 1998 and in revised form 12 March 1999.

References

1. Anderson, M.J., and M.W. Cohen. 1974. Fluorescent staining of acetylcholine receptors in vertebrate skeletal muscle. *J. Physiol. (Lond.)* 237:385–400.
2. Anderson, M.J., and M.W. Cohen. 1977. Nerve-induced and spontaneous redistribution of acetylcholine receptors on cultured muscle cells. *J. Physiol. (Lond.)* 268:757–773.
3. Anderson, M.J., and D.M. Fambrough. 1983. Aggregates of acetylcholine receptors are associated with plaques of a basal lamina heparan sulfate proteoglycan on the surface of skeletal muscle fibers. *J. Cell Biol.* 97: 1396–1411.
4. Anglister, L., J. Eichler, M. Szabo, B. Haesaert, and M.M. Salpeter. 1998. ^{125}I-labeled fasciculin 2: a new tool for quantitation of acetylcholinesterase densities at synaptic sites by EM-autoradiography. *J. Neurosci. Methods* 81:63–71.
5. Anglister, L., J.R. Stiles, and M.M. Salpeter. 1994. Acetylcholinesterase density and turnover number at frog neuromuscular junctions, with modeling of their role in synaptic function. *Neuron.* 12:783–794.
6. Bayne, E.K., M.J. Anderson, and D.M. Fambrough. 1984. Extracellular matrix organization in developing muscle: correlation with acetylcholine receptor aggregates. *J. Cell Biol.* 99:1486–1501.
7. Betz, W., and B. Sakmann. 1973. Effects of proteolytic enzymes on function and structure of frog neuromuscular junctions. *J. Physiol. (Lond.)* 230:673–688.
8. Bloch, R.J., and D.W. Pumplin. 1988. Molecular events in synaptogenesis: nerve-muscle adhesion and postsynaptic differentiation. *Am. J. Physiol.* 254:C345–C364.
9. Bourne, Y., P. Taylor, and P. Marchot. 1995. Acetylcholinesterase inhibition by fasciculin: crystal structure of the complex. *Cell.* 83:503–512.
10. Bowe, M.A., and J.R. Fallon. 1995. The role of agrin in synapse formation. *Annu. Rev. Neurosci.* 18:443–462.
11. Bowe, M.A., K.A. Deyst, J.D. Leszyk, and J.R. Fallon. 1994. Identification and purification of an agrin receptor from *Torpedo* postsynaptic membranes: A heteromeric complex related to the dystroglycans. *Neuron.* 12: 1173–1180.
12. Campanelli, J.T., S.L. Roberds, K.P. Campbell, and R.H. Scheller. 1994. A role for dystrophin-associated glycoproteins and utrophin in agrin-induced AChR clustering. *Cell.* 77:663–674.
13. Chen, Q., R. Sealock, and H.B. Peng. 1990. A protein homologous to the *Torpedo* postsynaptic 58K protein is present at the myotendinous junction. *J. Cell Biol.* 110:2061–2071.
14. Cohen, M.W., C. Jacobson, E.W. Godfrey, K.P. Campbell, and S. Carbonetto. 1995. Distribution of a-dystroglycan during embryonic nerve-muscle synaptogenesis. *J. Cell Biol.* 129:1093–1101.
15. Cohen, M.W., C. Jacobson, P.D. Yurchenco, G.E. Morris, and S. Carbonetto. 1997. Laminin-induced clustering of dystroglycan on embryonic muscle cells: comparison with agrin-induced clustering. *J. Cell Biol.* 136: 1047–1058.
16. Couteaux, R. 1955. Localization of cholinesterase at neuromuscular junctions. *In* International Review of Cytology. G.H. Bourne and J.F. Danielli, editors. Academic Press, New York. 335–375.
17. Deconinck, A.E., J.A. Rafael, J.A. Skinner, S.C. Brown, A.C. Potter, L. Metzinger, D.J. Watt, J.G. Dickson, J.M. Tinsley, and K.E. Davies. 1997. Utrophin-dystrophin-deficient mice as a model for Duchenne muscular dystrophy. *Cell.* 90:717–727.
18. Deprez, P.N., and N.C. Inestrosa. 1995. Two heparin-binding domains are present on the collagenic tail of asymmetric acetylcholinesterase. *J. Biol. Chem.* 270:11043–11046.
19. Eastman, J., E.J. Wilson, C. Cervenansky, and T.L. Rosenberry. 1995. Fasciculin 2 binds to the peripheral site on acetylcholinesterase and inhibits substrate hydrolysis by slowing a step involving proton transfer during enzyme acylation. *J. Biol. Chem.* 270:19694–19701.
20. Edwards, C., and H.L. Frisch. 1976. A model for the localization of acetylcholine receptors at the muscle endplate. *J. Neurobiol.* 7:377–381.
21. Fertuck, H.C., and M.M. Salpeter. 1974. Localization of acetylcholine receptor by ^{125}I-labeled a-bungarotoxin binding at mouse motor endplates. *Proc. Natl. Acad. Sci. USA.* 71:1376–1378.
22. Gee, S.H., F. Montanaro, M.H. Lindenbaum, and S. Carbonetto. 1994. Dystroglycan-α, a dystrophin-associated glycoprotein, is a functional agrin receptor. *Cell.* 77:675–686.
23. Grady, R.M., H.B. Teng, M.C. Nichol, J.C. Cunningham, R.S. Wilkinson, and J.R. Sanes. 1997. Skeletal and cardiac myopathies in mice lacking utrophin and dystrophin: a model for Duchenne muscular dystrophy. *Cell.* 90:729–738.
24. Hall, Z.W., and R.B. Kelly. 1971. Enzymatic detachment of endplate acetylcholinesterase from muscle. *Nat. New Biol.* 232:62–63.
25. Hall, Z.W., and J.R. Sanes. 1993. Synaptic structure and development: The neuromuscular junction. *Neuron.* 10(Suppl):99–121.
26. Harel, M., G.J. Kleywegt, R.B. Ravelli, I. Silman, and J.L. Sussman. 1995. Crystal structure of an acetylcholinesterase-fasciculin complex: interaction of a three-fingered toxin from snake venom with its target. *Structure.* 3:1355–1366.
27. Hassell, J.R., P.G. Robey, H.J. Barrach, J. Wilczek, S.I. Rennard, and G.R. Martin. 1980. Isolation of a heparan sulfate-containing proteoglycan from basement membrane. *Proc. Natl. Acad. Sci. USA.* 77:4494–4498.
28. Henry, M.D., and K.P. Campbell. 1996. Dystroglycan: an extracellular matrix receptor linked to the cytoskeleton. *Curr. Opin. Cell Biol.* 8:625–631.
29. Henry, M.D., and K.P. Campbell. 1998. A role for dystroglycan in basement membrane assembly. *Cell.* 95:859–870.
30. Inestrosa, N.C., and A. Perelman. 1989. Distribution and anchoring of mo-

lecular forms of acetylcholinesterase. *Trends Pharmacol. Sci.* 10:325–329.
31. Iozzo, R.V. 1994. The biology of perlecan: the multifaceted heparan sulphate proteoglycan of basement membrane and pericellular matrices. *Biochem. J.* 302:625–639.
32. Iozzo, R.V., and A.D. Murdoch. 1996. Proteoglycans of the extracellular environment: clues from the gene and protein side offer novel perspectives in molecular diversity and function. *FASEB J.* 10:598–614.
33. Johnson, C.D., and R.L. Russell. 1975. A rapid, simple radiometric assay for cholinesterase, suitable for multiple determinations. *Anal. Biochem.* 64:229–238.
34. Karlsson, E., P.M. Mbugua, and D. Rodriguez-Ithurralde. 1984. Fasciculins, anticholinesterase toxins from the venom of the green mamba Dendroaspis angusticeps. *J. Physiol. (Paris)* 79:232–240.
35. Kidokoro, Y., and B. Brass. 1985. Redistribution of acetylcholine receptors during neuromuscular junction formation in *Xenopus* cultures. *J. Physiol. (Paris)* 80:212–220.
36. Krejci, E., S. Thomine, N. Boschetti, C. Legay, J. Sketelj, and J. Massoulié. 1997. The mammalian gene of acetylcholinesterase-associated collagen. *J. Biol. Chem.* 272:22840–22847.
37. Ledbetter, S.R., L.W. Fisher, and J.R. Hassell. 1987. Domain structure of the basement membrane heparan sulfate proteoglycan. *Biochemistry.* 26: 988–995.
38. Lieth, E., and J.R. Fallon. 1993. Muscle agrin: neural regulation and localization at nerve-induced acetylcholine receptor clusters. *J. Neurosci.* 13: 2509–2514.
39. Lim, L.E., and K.P. Campbell. 1998. The sarcoglycan complex in limb-girdle muscular dystrophy. *Curr. Opin. Neurol.* 11:443–452.
40. Loeb, J.A., and G.D. Fischbach. 1995. ARIA can be released from extracellular matrix through cleavage of a heparin-binding domain. *J. Cell Biol.* 130:127–135.
41. Lubinska, L., and J. Zelena. 1967. Acetylcholinesterase at muscle-tendon junctions during postnatal development in rats. *J. Anat.* 101:295–308.
42. Malmqvist, M. 1997. Biospecific interaction analysis using biosensor technology. *Nature.* 361:186–187.
43. Massoulié, J., L. Pezzementi, S. Bon, E. Krejci, and F.-M. Vallette. 1993. Molecular and cellular biology of cholinesterases. *Prog. Neurobiol.* 41: 31–91.
44. McMahan, U.J., J.R. Sanes, and L.M. Marshall. 1978. Cholinesterase is associated with the basal lamina at the neuromuscular junction. *Nature.* 271:172–174.
45. Murdoch, A.D., B. Liu, R. Schwarting, R.S. Tuan, and R.V. Iozzo. 1994. Widespread expression of perlecan proteoglycan in basement membranes and extracellular matrices of human tissues as detected by a novel monoclonal antibody against domain III and by in situ hybridization. *J. Histochem. Cytochem.* 42:239–249.
46. Peng, H.B., and Q. Chen. 1992. Induction of dystrophin localization in cultured *Xenopus* muscle cells by latex beads. *J. Cell Sci.* 103:551–563.
47. Peng, H.B., L.P. Baker, and Q. Chen. 1991. Tissue culture of *Xenopus* neurons and muscle cells as a model for studying synaptic induction. *Methods Cell Biol.* 36:511–526.
48. Peng, H.B., D.-Y. Zhao, M.-Z. Xie, Z. Shen, and K. Jacobson. 1989. The role of lateral migration in the formation of acetylcholine receptor clusters induced by basic polypeptide-coated latex beads. *Dev. Biol.* 131:197–206.
49. Peng, H.B., A.A. Ali, Z. Dai, D.F. Daggett, E. Raulo, and H. Rauvala. 1995. The role of heparin-binding growth-associated molecule (HB-GAM) in the postsynaptic induction in cultured muscle cells. *J. Neurosci.* 15:3027–3038.
50. Peng, H.B., A.A. Ali, H. Rauvala, J.R. Hassell, and N.R. Smalheiser. 1998. The relationship between perlecan and dystroglycan and its implication in the formation of the neuromuscular junction. *Cell Adhesion Commun.* 5:475–489.
51. Rogalski, T.M., B.D. Williams, G.P. Mullen, and D.G. Moerman. 1993. Products of the unc-52 gene in *Caenorhabditis elegans* are homologous to the core protein of the mammalian basement membrane heparan sulfate proteoglycan. *Genes Dev.* 7:1471–1484.
52. Rossi, S.G., and R.L. Rotundo. 1993. Localization of "non-extractable" acetylcholinesterase to the vertebrate neuromuscular junction. *J. Biol. Chem.* 268:19152–19159.
53. Rossi, S.G., and R.L. Rotundo. 1996. Transient interactions between collagen-tailed acetylcholinesterase and sulfated proteoglycans prior to immobilization on the extracellular matrix. *J. Biol. Chem.* 271:1979–1987.
54. Rotundo, R.L. 1984. Purification and properties of the membrane-bound form of acetylcholinesterase from chicken brain. *J. Biol. Chem.* 259: 13186–13194.
55. Rotundo, R.L. 1984. Asymmetric acetylcholinesterase is assembled in the Golgi apparatus. *Proc. Natl. Acad. Sci. USA.* 81:479–483.
56. Rotundo, R.L., S.G. Rossi, and L. Anglister. 1997. Transplantation of quail collagen-tailed acetylcholinesterase molecules onto the frog neuromuscular synapse. *J. Cell Biol.* 136:367–374.
57. Sanes, J.R., M. Schachner, and J. Covault. 1986. Expression of several adhesive macromolecules (N-CAM, L1, J1, NILE, uvomorulin, laminin, fibronectin, and a heparan sulfate proteoglycan) in embryonic, adult, and denervated adult skeletal muscle. *J. Cell Biol.* 102:420–431.
58. Sugiyama, J., D.C. Bowen, and Z.W. Hall. 1994. Dystroglycan binds nerve and muscle agrin. *Neuron.* 13:103–115.
59. Yurchenco, P.D., and J.C. Schittny. 1990. Molecular architecture of basement membranes. *FASEB J.* 4:1577–1590.